

PROBING DARK ABELIAN GAUGE SECTOR AT THE INTENSITY FRONTIER

Gabriel Massoni Salla

Instituto de Física, Universidade de São Paulo, C.P. 66.318, 05315-970 São Paulo, Brazil

Abstract

In this study we explore the phenomenology of an UV complete dark photon model, in which we explicitly consider a new scalar sector responsible for the mass generation. In this context, we compute the present and future sensitivity regions for KOTO, LHCb and Belle II by considering meson decays to 4-lepton final states. We find that these experiments have large sensitivity to this model and that, under some circumstances, the connection between the dark photon and the scalar sector can completely change the low-energy phenomenology of both.

1 Introduction

Models containing new vector fields associated to new gauge symmetries are among the best motivated extensions of the Standard Model (SM). In particular, a large class of beyond the SM (BSM) models predict the existence of a new $U(1)_D$ gauge symmetry with a massive gauge boson at low-energies (see Ref. 1) for a recent review). In most studies it is assumed that this vector field has a Stückelberg mass, thus making the model incomplete and possibly ill-defined in the UV. This owns to the lack of a mass generation mechanism for the new gauge boson and the presence of potentially non-vanishing operators that induce a bad high-energy behaviour 2). In the present study, instead, we consider an UV complete scenario, in which the simplest mass generation mechanism is responsible for the mass of the new gauge boson 3). We then predict how the standard phenomenology of the model with a Stückelberg mass is modified in this new context by analysing meson decay signatures at KOTO 4), LHCb 5) and Belle II 6) experiments. For a complete discussion and more details on the analysis, we refer the reader to Ref. 7).

2 UV complete Dark Photon model

Our starting point is the most general renormalizable Lagrangian for a massless gauge boson Z_D , named here dark photon

$$\mathcal{L}_{\text{vector}} = -\frac{1}{4}Z_{D\mu\nu}Z_D^{\mu\nu} + \frac{\epsilon}{2}Z_D^{\mu\nu}B_{\mu\nu}, \quad (1)$$

with ϵ the kinetic mixing parameter¹. Notice that we consider all SM particles to be neutral under the new symmetry group. The mass generation proceeds via a dark Higgs mechanism, in which a new scalar field S , the dark Higgs, spontaneously breaks $U(1)_D$. The Lagrangian for the scalar sector reads

$$\mathcal{L}_{\text{scalar}} = |D_\mu H|^2 + |D_\mu S|^2 - V(H, S), \quad (2)$$

with H the SM-like Higgs boson and

$$V(H, S) = m_H^2|H|^2 + \lambda|H|^4 + m_S^2|S|^2 + \lambda_S|S|^4 + \kappa|H|^2|S|^2. \quad (3)$$

The dark Higgs is supposed to be a SM-singlet, such that $D_\mu S = \partial_\mu S + ig_D Z_{D\mu} S$, with g_D the $U(1)_D$ gauge coupling. After both scalars pick up a vacuum expectation value (vev), we have four effects:

- The kinetic mixing term in Eq. (1), after diagonalization of kinetic and mass terms, generates a coupling between the dark photon Z_D and the electromagnetic current suppressed by a factor ϵ . This result holds as long as $\epsilon \ll 1$ and $m_{Z_D} \ll v$, v being the electroweak vev, which is precisely the region of interest;
- The quartic term $\kappa|H|^2|S|^2$ induces a mass mixing between both scalars. Up to first order in the couplings, the physical mixing angle is given by

$$s_h \simeq \frac{\kappa v_S v}{m_s^2 - m_h^2}, \quad (4)$$

where v_S is the vev of S and $m_{h,s}$ are the masses of the physical scalars h, s after the diagonalization. As a direct consequence of this mixing, the dark Higgs s inherits all interactions of the SM-like Higgs, suppressed, however, by a power of s_h ;

- The kinetic term of the dark Higgs produces a mass term for the dark photon, namely $m_{Z_D} = g_D v_S$;
- In addition to the dark photon mass, the kinetic term $|D_\mu S|^2$ contains an interaction between the dark particles given by

$$|D_\mu S|^2 \supset g_D m_{Z_D} s Z_{D\mu} Z_D^\mu. \quad (5)$$

The interactions of the Z_D field with the electromagnetic current and the scalar mixing are precisely what characterises the usual dark photon and dark Higgs phenomenology, respectively^{1, 9)}. The $U(1)_D$ gauge connection in Eq. (5) brings together both scalar and vector sectors and can thus give rise to novel phenomenological signatures. If we take $g_D \rightarrow 0$ while maintaining m_{Z_D} constant, we decouple both sectors and recover the usual phenomenology for both models. Hence, in order to study the effects of the dark gauge connection (5), we need to assume that its strength is at least comparable to the other interactions².

¹A tiny kinetic mixing ranging in $10^{-2} < \epsilon < 10^{-13}$ can be obtained through multi-loop processes in theories where the tree-level is forbidden in the UV⁸⁾.

²Here we neglect the decays of S to a photon and a dark photon that take place via the kinetic mixing, as the width is further suppressed by ϵ^2 .

One of the main features of Eq. (5) is to give a contribution to the dark Higgs decay width that is independent of s_h^2 . The partial width $\Gamma(s \rightarrow Z_D Z_D)$ is proportional to g_D^2 and is parametrically larger than the decay rates inherited from the SM-like Higgs that scale with s_h^2 . More precisely, the branching ratio to a pair of dark photons will be approximately 1 if $g_D \gg 7 \cdot 10^{-3} s_h$ is satisfied. While most dark Higgs searches rely on the dark Higgs decaying to pairs of fermions⁹⁾, the scenario in which this hierarchy is respected allow us to probe directly the gauge structure of the $U(1)_D$ group. For this reason we focus our phenomenological analysis on the channel $s \rightarrow Z_D Z_D$.

3 Phenomenology

In order to probe the decay $s \rightarrow Z_D Z_D$ in a real experiment, we must first produce the dark Higgs. This can be achieved through the scalar mixing, in which a SM particle, in our case a meson, decays to s plus other SM states³. The corresponding branching ratio will turn out to be small considering that s_h is expected to be small. To compensate for this, we can profit from experiments at the high intensity frontier, *i.e.* experiments that will take large amounts of data and perform very precise measurements. In particular, the KOTO, LHCb and Belle II experiments aim to probe, respectively, extremely rare kaons, B -mesons and Υ 's decays with increasing luminosity in the years to come.

3.1 Visible signatures - LHCb and Belle II

In LHCb and Belle II we consider $B^\pm \rightarrow K + s$, with K a kaon state, and $\Upsilon(1S, 2S, 3S) \rightarrow \gamma + s$ respectively^{9, 11)}. The number of events expected in these experiments is given by the formula

$$N_{\text{evt}} = N_M \text{ BR}(M \rightarrow s + M') \text{ BR}(s \rightarrow Z_D Z_D) P_{\text{dec}}^{\text{in}} f_{\text{geom}} \text{ BR}(Z_D \rightarrow \ell^- \ell^+)^2 \varepsilon, \quad (6)$$

where M (M') = B^\pm (K) or Υ (γ), N_M is the total number of mesons produced, $P_{\text{dec}}^{\text{in}}$ is the probability of the dark photons to decay inside the experimental volume⁴, f_{geom} is the geometrical acceptance and ε is the particle detection efficiency. In the equation above we take both dark photons to be decaying into a pair of charged leptons, which implies that the experimental signature involves a 4-lepton final state. Since we demand all final states to be observed within the detector, the signature given by Eq. (6) is denoted as *visible*.

In both LHCb and Belle II cases we might have background coming from the SM. Since the SM backgrounds decay promptly, we can rely on the long-lived nature of the dark particles and require the signal to be displaced, in other words, demand that the dark particles are enough long-lived such that they decay some distance away from the initial vertex. In this manner one can univocally disentangle the signal from the background. The definition of a displaced signal depends on the spatial resolution of the vertex detector of each experiment. For LHCb we use 0.82 cm, while for Belle II we use 3.8 cm. The situation is more complicated if the dark particles decay promptly, but background can still be avoided if either the decay rate of the model is expected to be much larger than the SM one (approximately for $s_h > 10^{-3}$ in the case of LHCb and $s_h > 10^{-2}$ for Belle II), or by searching for resonances in di-lepton invariant masses, which are characteristic of the decay chain $s \rightarrow Z_D Z_D \rightarrow 4\ell$.

³Measurements of the Higgs coupling strength imposes that $s_h < 0.1$ ¹⁰⁾.

⁴We consider throughout our analysis that $g_D > 10^{-3}$. For such values the dark Higgs decays promptly in all experiments considered, that is, with decay length less than the corresponding spatial resolution. Whence, all decay probabilities refer to the dark photons only.

To compute the number of events in Eq. (6) we simulated the initial meson flux with **Pythia8**¹²⁾ and computed the decay probability with **MadDump**¹³⁾, using the **UFO** model of Ref. 3). For LHCb we use that the angular acceptance is $2 < \eta < 5$ and that the maximum baseline of the detector is 20 m. Moreover, we use the combined luminosities of Run 1 and 2 of 9 fb^{-1} , meaning that about 10^{11} B 's were produced. For Belle II we consider the detector to be a cylinder of radius of 3.48 m and length 7.38 m, while the angular acceptance is given by $17^\circ < \theta < 150^\circ$ with respect to the dislocated collision point. We assume here that Belle II will produce approximately 40 times more Υ 's than Belle, which is equivalent to $4 \times 10^9 \Upsilon(1S)$, $6.3 \times 10^9 \Upsilon(2S)$ and $4.8 \times 10^8 \Upsilon(3S)$ events.

In Fig. 1 we show the sensitivity regions in the dark photon and dark Higgs parameter spaces corresponding to $N_{\text{evts}} \geq 3$. We see in general that the regions we obtain in our case are significantly different from the ones obtained considering either only the dark photon or only the dark Higgs, meaning that the dark gauge coupling can indeed affect the phenomenology of both particles. In the left panel of Fig. 1, the lines crossing the regions denote when the dark photons have a particular decay length, which are then used to define whether a signal is displaced or not. Also, we end up being sensitive to much smaller values of ϵ due to the fact that in Eq. (6) the total number of dark photons produced does not depend on the kinetic-mixing, thus de-correlating production and detection.

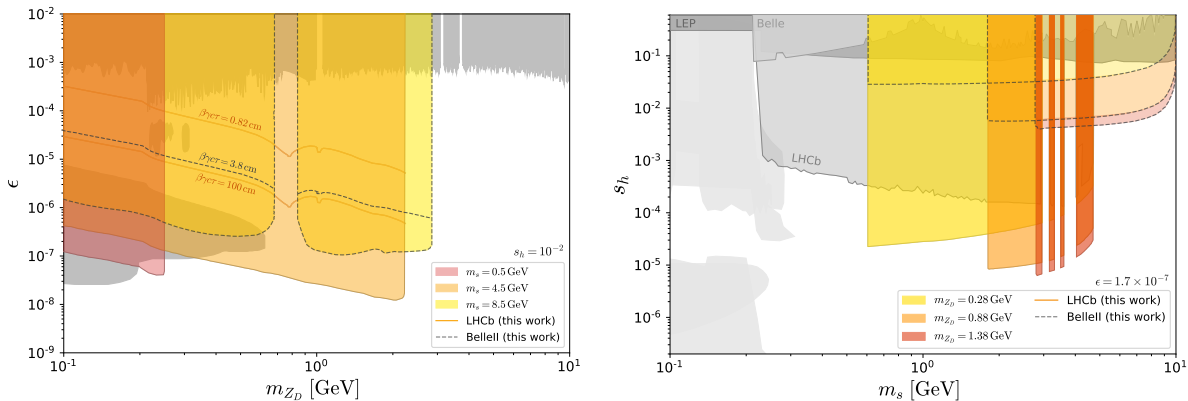


Figure 1: *Left)* Expected sensitivity in the $m_{Z_D} \times \epsilon$ parameter space for the LHCb (solid) and Belle II (dashed) searches. We fix $s_h = 10^{-2}$. The solid orange (dashed black) line crossing LHCb (Belle II) bounds indicate where the dark photon decay length reaches 0.82 cm (3.8 cm), which is the spatial resolution of the detector's vertex locator. We also indicate $\beta\gamma\tau = 100 \text{ cm}$ for LHCb, corresponding to when dark photons start to exit the vertex detector. *Right)* Expected bounds in the $m_s \times s_h$ plane for the LHCb search (solid) and the future sensitivity projection for the Belle II search (dashed). We fixed the kinetic mixing parameter to $\epsilon = 1.7 \times 10^{-7}$. The vetoed regions represent the meson resonances that we have considered as irreducible backgrounds. In both plots the gray regions denote limits from searches for dark photons and dark Higgs in the limit they are decoupled.

3.2 Invisible signatures - KOTO

The situation in KOTO is very different from LHCb and Belle II. The main goal of the collaboration is to measure the CP-violating decay $K_L \rightarrow \pi^0 \nu \bar{\nu}$. Latest measurements can set an upper bound on the respective branching ratio, given by $\text{BR}(K_L \rightarrow \pi^0 X) < 3.7 \cdot 10^{-9}$ for X invisible¹⁴⁾. Note that X in this case must be necessarily invisible to the detector, so to mimic the neutrinos in the SM decay. Therefore, the bound from KOTO can be translated to a bound on the model parameter space if the dark photons

decay outside the detector, which can be quantified by the effective branching ratio

$$\text{BR}_{\text{eff}} \equiv \text{BR}(K_L \rightarrow \pi^0 s) \text{BR}(s \rightarrow Z_D Z_D) P_{\text{dec}}^{\text{out}}, \quad (7)$$

where now $P_{\text{dec}}^{\text{out}}$ is the probability of the dark photons to escape the detector, as opposed to $P_{\text{dec}}^{\text{in}}$ in Eq. (6). The branching ratio for $K_L \rightarrow \pi^0 s$ was taken from Ref. 15).

To estimate the effective branching ratio of Eq. (7) we simulate a K_L flux according to Ref. 16) with approximately $6.4 \cdot 10^{12}$ kaons produced and consider the decay volume used in Refs. 14, 17). Our results are presented in Fig. 2, in which we show the regions in the dark photon (left panel) and dark Higgs (right panel) parameter space that are excluded by demanding that $\text{BR}_{\text{eff}} \leq \text{BR}(K_L \rightarrow \pi^0 X)$. We note that in the $m_s \times s_h$ parameter space we lose sensitivity as the kinetic-mixing grows and saturates as $\epsilon < 10^{-6}$. In the dark photon parameter space we can achieve a much larger sensitivity due to the fact that BR_{eff} depends on ϵ and m_{Z_D} solely through $P_{\text{dec}}^{\text{out}}$. As a consequence, the experiment is sensitive to lower and lower values of kinetic-mixing and mass, as in this region the dark photons are more long-lived and thus escape more often the KOTO detector⁵.

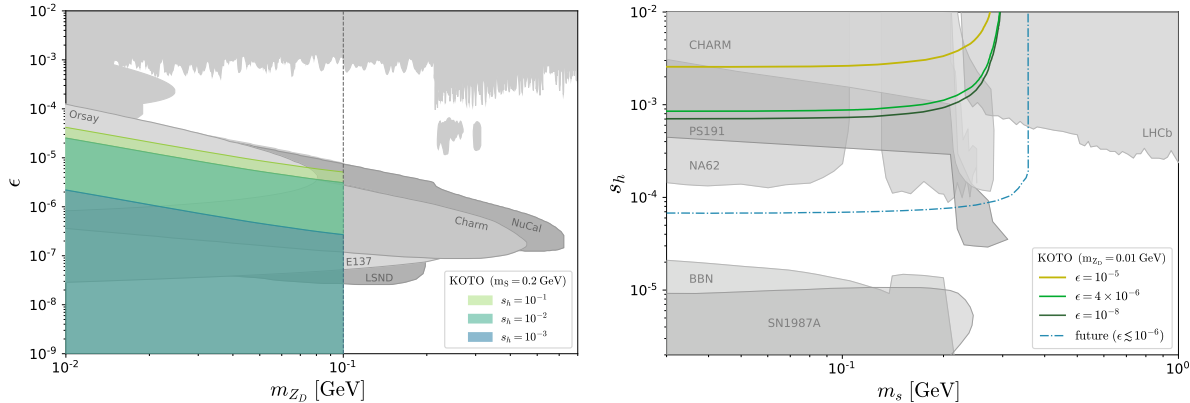


Figure 2: Left) Limits from KOTO translated to the dark photon parameter space, where we have fixed $m_s = 0.2$ GeV and colored regions are excluded for $s_h = 10^{-1}$ (green), 10^{-2} (blue) and 10^{-3} (dark blue). The regions extend down to $\epsilon = 0$. Right) Current bounds on the dark Higgs parameter space coming from KOTO fixing $m_{Z_D} = 0.01$ GeV. The different solid curves consider $\epsilon = 10^{-5}$ (yellow), 4×10^{-6} (green) and 10^{-8} (dark green). We show in blue dashed-dotted the maximum future sensitivity of the KOTO experiment assuming the SM prediction for $\text{BR}(K_L \rightarrow \pi^0 \nu \bar{\nu})$ can be attained. Gray regions are the same from Fig. 1.

4 Discussion and conclusions

In this work we have addressed the question whether or not the consideration of an explicit mass generation mechanism for the simplest dark photon model can impact its low-energy phenomenology. Indeed, we find that under some assumptions the dark gauge connection can dramatically modify experimental searches for dark photons and dark Higgs. We have seen this explicitly by considering 4-lepton final state decays of K_L , B^\pm and Υ 's at KOTO, LHCb and Belle II. Taking into account present and future data for

⁵Analogously, upper bounds on the SM Higgs invisible width can put bounds on the $m_{Z_D} \times \epsilon$ plane that are similar to those obtained for the KOTO experiment 7).

these experiments, we see great prospects of probing interesting and very unique regions of the parameter space.

Acknowledgements

The author acknowledges financial support from Fundação de Amparo à Pesquisa de São Paulo (FAPESP) under contract 2020/14713-2 and partial financial support from the school organization to attend the XX LNF Summer School “Bruno Touschek” in Nuclear, Subnuclear and Astroparticle Physics.

References

1. M. Fabbrichesi, E. Gabrielli and G. Lanfranchi, doi:10.1007/978-3-030-62519-1 [arXiv:2005.01515 [hep-ph]].
2. G. D. Kribs, G. Lee and A. Martin, Phys. Rev. D **106**, no.5, 055020 (2022) doi:10.1103/PhysRevD.106.055020 [arXiv:2204.01755 [hep-ph]].
3. D. Curtin, R. Essig, S. Gori and J. Shelton, JHEP **02** (2015), 157 doi:10.1007/JHEP02(2015)157 [arXiv:1412.0018 [hep-ph]].
4. T. Yamanaka [KOTO], PTEP **2012** (2012), 02B006 doi:10.1093/ptep/pts057
5. A. A. Alves, Jr. *et al.* [LHCb], JINST **3** (2008), S08005 doi:10.1088/1748-0221/3/08/S08005
6. T. Abe *et al.* [Belle-II], [arXiv:1011.0352 [physics.ins-det]].
7. A. L. Foguel, G. M. Salla and R. Z. Funchal, [arXiv:2209.03383 [hep-ph]].
8. T. Gherghetta, J. Kersten, K. Olive and M. Pospelov, Phys. Rev. D **100**, no.9, 095001 (2019) doi:10.1103/PhysRevD.100.095001 [arXiv:1909.00696 [hep-ph]].
9. M. W. Winkler, Phys. Rev. D **99** (2019) no.1, 015018 doi:10.1103/PhysRevD.99.015018 [arXiv:1809.01876 [hep-ph]].
10. R. L. Workman [Particle Data Group], PTEP **2022** (2022), 083C01 doi:10.1093/ptep/ptac097
11. F. Wilczek, Phys. Rev. Lett. **39** (1977), 1304 doi:10.1103/PhysRevLett.39.1304
12. T. Sjostrand, S. Mrenna and P. Z. Skands, Comput. Phys. Commun. **178** (2008), 852-867 doi:10.1016/j.cpc.2008.01.036 [arXiv:0710.3820 [hep-ph]].
13. L. Buonocore, C. Frugiuele, F. Maltoni, O. Mattelaer and F. Tramontano, JHEP **05** (2019), 028 doi:10.1007/JHEP05(2019)028 [arXiv:1812.06771 [hep-ph]].
14. J. Liu, N. McGinnis, C. E. M. Wagner and X. P. Wang, JHEP **04** (2020), 197 doi:10.1007/JHEP04(2020)197 [arXiv:2001.06522 [hep-ph]].
15. H. Leutwyler and M. A. Shifman, Nucl.Phys.B**343**(1990), 369-397 doi:10.1016/0550-3213(90)90475-S
16. K. Shiomi *et al.* [KOTO], Nucl. Instrum. Meth. A **664** (2012), 264-271 doi:10.1016/j.nima.2011.11.010
17. J. K. Ahn *et al.* [KOTO], Phys. Rev. Lett. **126** (2021) no.12, 121801 doi:10.1103/PhysRevLett.126.121801 [arXiv:2012.07571 [hep-ex]].